Original Article

Identification of immune-related prognostic biomarkers in triple-negative breast cancer

Xiao-Qing Song[1,2], Zhi-Ming Shao[1,2]

[1]Key Laboratory of Breast Cancer in Shanghai, Department of Breast Surgery, Fudan University Shanghai Cancer Center, Shanghai, China; [2]Department of Oncology, Shanghai Medical College, Fudan University, Shanghai, China

Contributions: (I) Conception and design: XQ Song; (II) Administrative support: XQ Song; (III) Provision of study materials or patients: XQ Song; (IV) Collection and assembly of data: XQ Song; (V) Data analysis and interpretation: XQ Song; (VI) Manuscript writing: Both authors; (VII) Final approval of manuscript: Both authors.

Correspondence to: Zhi-Ming Shao, MD. Key Laboratory of Breast Cancer in Shanghai, Department of Breast Surgery, Fudan University Shanghai Cancer Center, No. 270 Dong'an Road, Shanghai 200032, China; Department of Oncology, Shanghai Medical College, Fudan University, Shanghai, China. Email: zhi_ming_shao@163.com.

Background: Triple-negative breast cancer (TNBC), a type of breast cancer, lacks immune-related markers that can be used for prognosis or prediction. Therefore, we created a predictive framework for TNBC using a risk assessment.

Methods: Our previous study group consisted of 360 individuals who were diagnosed with TNBC through pathology using RNA sequencing and had clinical data from Fudan University Shanghai Cancer Center (FUSCC). A risk scoring model was constructed using the Cox regression method with the least absolute shrinkage and selection operator (LASSO). A multivariate Cox regression analysis was utilized to develop the prediction model, which was then assessed using the consistency index and calibration plots. The validation cohort of The Cancer Genome Atlas (TCGA) TNBC confirmed the strength of the signatures' predictive value.

Results: The prognostic risk score model included 12 genes: *TDO2*, *CHIT1*, *CARML2*, *HLA-C*, *ADIRF*, *C19orf33*, *CA8*, *AHNAK2*, *RHOV*, *OPLAH*, *THEM6*, and *NEBL*. The receiver operator characteristic (ROC) curves for survivability values at 1, 3, and 5 years in the FUSCC TNBC cohort demonstrated area under the curve (AUC) values of 0.78, 0.83, and 0.75, respectively. These results indicated a high level of accuracy in predicting outcomes, which was further confirmed through validation using TCGA database. The patients in the high-risk group showed worse prognoses and lower levels of immune cell infiltration, specifically $CD8^+$ T cells, than those in the low-risk group. Furthermore, the low-risk group exhibited a significant upregulation of genes that encode immune checkpoints, including *CD274* and *CTLA4*, suggesting that immunotherapy may yield enhanced efficacy within this particular group.

Conclusions: In conclusion, the prognostic signature consisting of 12 genes can assist in the choice of immunotherapy for TNBC.

Keywords: Triple-negative breast cancer (TNBC); immune risk score; prognosis; biomarker

Submitted Aug 28, 2023. Accepted for publication Feb 29, 2024. Published online Apr 25, 2024.
doi: 10.21037/tcr-23-1554
View this article at: https://dx.doi.org/10.21037/tcr-23-1554

Introduction

Breast cancer is the most common lethal cancer in women (1,2). Triple-negative breast cancer (TNBC) is a distinct subset of breast cancer, accounting for approximately 15% of total occurrences. TNBC has a bleak outlook because of its high histological grade and aggressive behavior, which are not easy for the attainment of effective treatment (3). TNBC does not respond to conventional hormonal treatments and

is resistant to human epidermal growth factor receptor-2 (*HER2*)-targeted therapy. Additionally, chemotherapy and radiotherapy may not always provide effective treatment for TNBC (4-7). Thus, there is an urgent need to develop novel effective targeted therapies.

Studies based on clinical data and experiments have indicated that immunotherapy has the potential to significantly extend the lifespan of individuals. In recent years, several clinical studies have investigated immunotherapy treatments for TNBC (8-10). Compared to other subtypes, TNBC is considered to be sensitive to immunotherapy due to certain traits, such as genomic instability, a high tumor mutation burden, and elevated levels of immune infiltration (11,12). In addition, compared with other subtypes, TNBC patients exhibit significant expression of programmed cell death ligand 1 (*PD-L1*) (13). This discovery opens up new possibilities and guidelines for the advancement of effective immunotherapy treatments for TNBC patients (14). While TNBC exhibits a greater reaction to immune checkpoint inhibitors (ICIs) than other subtypes, there are TNBC patients who demonstrate limited effectiveness of immunotherapy (15). Hence, it is imperative to create innovative and efficient immune-associated indicators for forecasting the outcome and effectiveness of immunotherapy.

This study aimed to discover new prognostic biomarkers associated with the immune system. Initially, we discovered 2,008 genes that were expressed differently between the immunomodulatory (IM) group (n=87) and the remaining subtypes (n=273). Survival was significantly predicted by 33 immune-related genes (IRGs) according to the findings of univariate Cox regression analysis. Using the least absolute shrinkage and selection operator (LASSO) regression analysis, a model was created to predict breast cancer survival outcomes, including 12 out of 33 IRGs. A prognostic model was built and then validated in The Cancer Genome Atlas (TCGA) TNBC cohort. The identification of immune-related prognostic indicators for TNBC in our study aids in the precise immunotherapy of TNBC. We present this article in accordance with the TRIPOD reporting checklist (available at https://tcr.amegroups.com/article/view/10.21037/tcr-23-1554/rc).

Highlight box

Key findings

- A prognostic signature consisting of twelve genes can assist in the choice of immunotherapy for triple-negative breast cancer (TNBC).

What is known and what is new?

- TNBC lacks immune-related markers that can be used for prognosis or immunotherapy prediction.
- The prognostic model was found to be associated with the prognosis of TNBC patients and immunotherapy efficacy.

What is the implication, and what should change now?

- This study provided immune-related markers that can be used for prognosis or prediction.

Methods

Study cohort

Our previous study (16) described a total of 465 patients diagnosed with TNBC by pathology from Fudan University Shanghai Cancer Center (FUSCC) in the entire study cohort. The cohort contained 360 samples with RNA-sequencing data and 279 samples with whole exome sequencing (WES) data. All samples were previously untreated primary breast cancers. The study was conducted in accordance with the Declaration of Helsinki (as revised in 2013). The study was approved by the independent ethics committee at Fudan University Shanghai Cancer Center Ethical Committee (No. 2019171). Informed consent were obtained. Data on TNBC (n=145), including expression, mutation, and clinical information, were obtained by utilizing the TCGA database. We acquired the single-cell RNA sequencing (scRNA-seq) information of five TNBC individuals from the Gene Expression Omnibus (GEO) repository using the study identifier GSE148673.

Currently, there is an ongoing multicenter trial called I-SPY2, which is adaptively randomized and open-label in nature. The study examined the use of neoadjuvant chemotherapy (NACT) in treating early-stage breast cancer patients with a high risk of recurrence (NCT01042379) (17,18). The platform trial simultaneously evaluates multiple investigational arms, each comprising NACT as a common control arm, along with an investigational agent or combination. For women diagnosed with breast cancer, the main objective is achieving pathologic complete response (pCR), which means there are no invasive tumors present in the breast or nearby lymph nodes following surgical treatment. The current investigation assessed the expression of *TDO2*, *HLA-C*, and *OPLAH* as distinct indicators for predicting pCR to the combination of paclitaxel and pembrolizumab.

Identification of differentially expressed IRGs and survival-associated IRGs

We used the limma package in R to analyze differential expression. Differential expression analysis was carried out comparing the IM group (n=87) with the remaining subtypes (n=273). Genes that satisfied the filtering conditions of adjust P<0.05 and |Log2 fold change (FC)| >0.58 were categorized as genes exhibiting differential expression. Survival-associated IRGs were identified using univariate Cox regression analysis in R with the 'survival' package.

Perform GO and KEGG analyses

To elucidate the role of the dysregulated redox-associated genes, we utilized the R package 'clusterProfiler' to conduct enrichment analyses for Gene Ontology (GO) and Kyoto Encyclopedia of Genes and Genomes (KEGG) analyses. The *q* value and the P value were the selection criteria, which must be less than 0.05.

Development and verification of the IRG signature

To construct the most precise and feasible prediction model, one can utilize the LASSO technique, which assigns weights to model parameters and identifies the crucial variables. We performed LASSO Cox regression using the R package 'glmnet' (19). Based on the findings of this analysis, a model was created using a 12-gene signature to forecast clinical outcomes in patients with TNBC. For each sample, risk scores were calculated by using coefficients assigned to each prognostic IRG. Risk scores were used to classify patients into high- and low-risk groups during training and validation, which was determined using the median value.

Performance analysis

The survival package in R was utilized to analyze data concerning patients in the model. A log-rank test and Kaplan-Meier curves were employed to examine disparities between the two groups. The sensitivity and specificity of a model in predicting outcome events are often determined using a receiver operating characteristic curve (20). We utilized the R package 'survival' for the purpose of the receiver operator characteristic (ROC) analysis. Using the median risk score as a threshold, we plotted clinical outcome data against the risk score for patients with breast cancer. Our research produced ROC curves and computed the area under the curve (AUC) for survival at 3 and 5 years. Bootstrap resampling (1,000 resamplings) was utilized to assess the calibration capability of the nomograms. The line at a 45-degree angle symbolized ideal calibration, and the proximity of the line indicated the quality of calibration.

Estimation of immune infiltration

The CIBERSORT algorithm (21) was utilized to examine the infiltration of immune cells. The Wilcoxon rank-sum test was used to analyze the disparities in immune infiltrating cell scores between the low- and high-risk groups.

Mutation spectrum characteristics

The analysis involved utilizing genetic somatic mutation data from the FUSCC TNBC cohort to compare the disparities between low- and high-risk groups. The analysis of genetic mutation differences between low-risk and high-risk groups was conducted using Maftools (22).

Single-cell RNA-seq analysis

The t-distributed Stochastic Neighbor Embedding (tSNE) method was employed with the 'seurat' data processing package to decrease nonlinear dimensions (1). An annotated cell cluster was then created using the "singleR" package in combination with canonical markers (2). Additionally, the expression of genes in each cluster was plotted using the 'seurat' package.

Statistical analysis

The data were assessed for statistical significance using GraphPad Prism software version 8 (GraphPad Software, San Diego, CA, USA) and R software version 3.5.2. Recurrence-free survival (RFS) was defined as the period from surgery to recurrence or last follow-up. Plots were created to assess the patients' prognosis for 1-, 3-, and 5-year RFS using ROC curves. Survival analysis was performed using Kaplan-Meier with the Log-rank test. Student's *t*-test was used to compare the variances between two groups. Analysis items with P<0.05 were considered statistically significant.

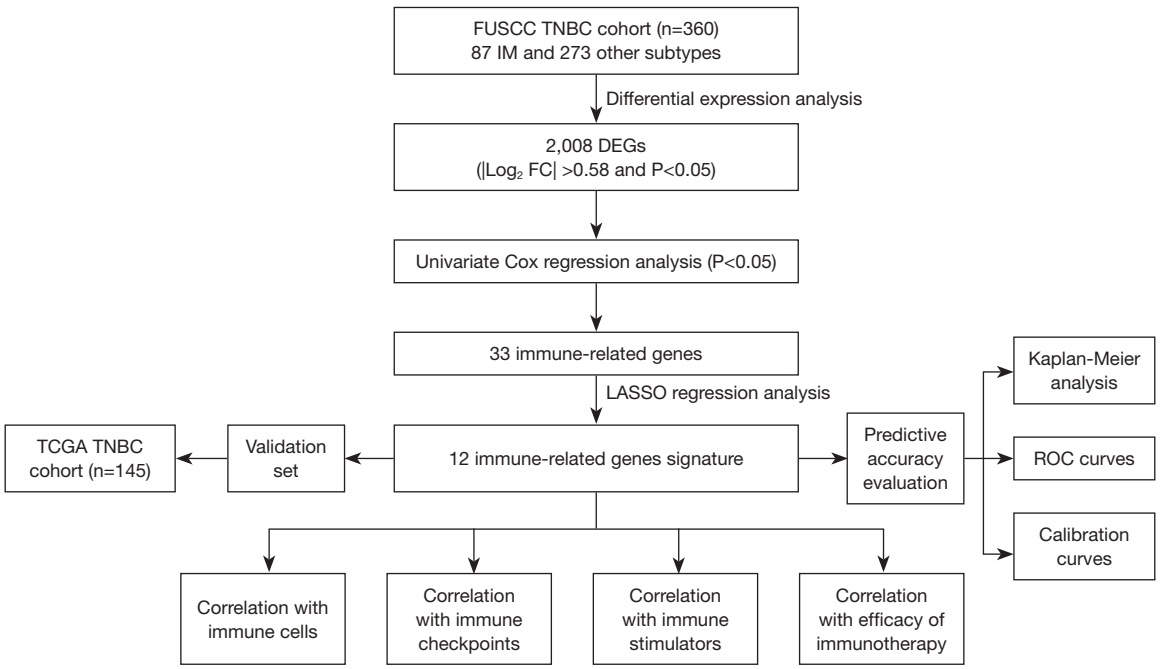

Figure 1 Schematic of the research strategy. FUSCC, Fudan University Shanghai Cancer Center; TNBC, triple-negative breast cancer; IM, immunomodulatory; DEGs, different expression genes; FC, fold change; LASSO, least absolute shrinkage and selection operator; TCGA, The Cancer Genome Atlas; ROC, receiver operator characteristic.

Results

IRG model construction

We identified a total of 2008 distinct genes with differential expression (P<0.05, |log FC| >0.58) between the IM subtype and the remaining subtypes (*Figures 1*,*2A*). Univariate Cox analysis was conducted to detect survival-associated IRGs, resulting in the identification of 33 genes as survival-related genes (*Figure 2B*). Afterwards, the implementation of LASSO Cox regression analysis led to the discovery of twelve genes associated with the immune system: *TDO2*, *CHIT1*, *CARMIL2*, *HLA-C*, *ADIRF*, *C19orf33*, *CA8*, *AHNAK2*, *RHOV*, *OPLAH*, *THEM6*, and *NEBL* (*Figure 2C*). We used these genes to establish a prognostic risk model. The risk score for each individual was computed using the following equation: risk score = [The expression of *TDO2* × (−0.13)] + [The expression of *CHIT1* × (−0.13)] + [The expression of *CARMIL2* × (−0.0004)] + [The expression of *HLA-C* × (−0.05)] + (The expression of *ADIRF* × 0.07) + (The expression of *C19orf33* × 0.07) + (The expression of *CA8* × 0.03) + (The expression of *AHNAK2* × 0.05) + (The expression of *RHOV* × 0.03) + (The expression of *OPLAH* × 0.006) + (The expression of *THEM6* × 0.16) + (The expression of *NEBL* × 0.16). After calculating their risk scores, the patients were divided into two groups based on whether their scores were above or below the median value.

We displayed the distribution of risk scores between the low-risk and high-risk groups in the training and validation sets (*Figure 3A*,*3B*). Next, we displayed the survival status and survival time of patients in various risk categories in both the training and validation sets (*Figure 3C*,*3D*). In addition, the expression levels of 12 immune-related prognostic genes were examined in both the training and validation sets for each patient, as shown in *Figure 3E*,*3F*. According to the findings, patients who experienced recurrence exhibited elevated risk scores (*Figure 3G*). The analysis of survival indicated that participants classified as high-risk experienced a lower rate of RFS than those classified as low-risk (FUSCC TNBC cohort, P=0.001; TCGA TNBC cohort, P=0.005) (*Figure 3H*).

Validation of the prognostic risk model

By integrating the risk score with the pathologic T and N stage, we constructed a nomogram (*Figure 4A*). When

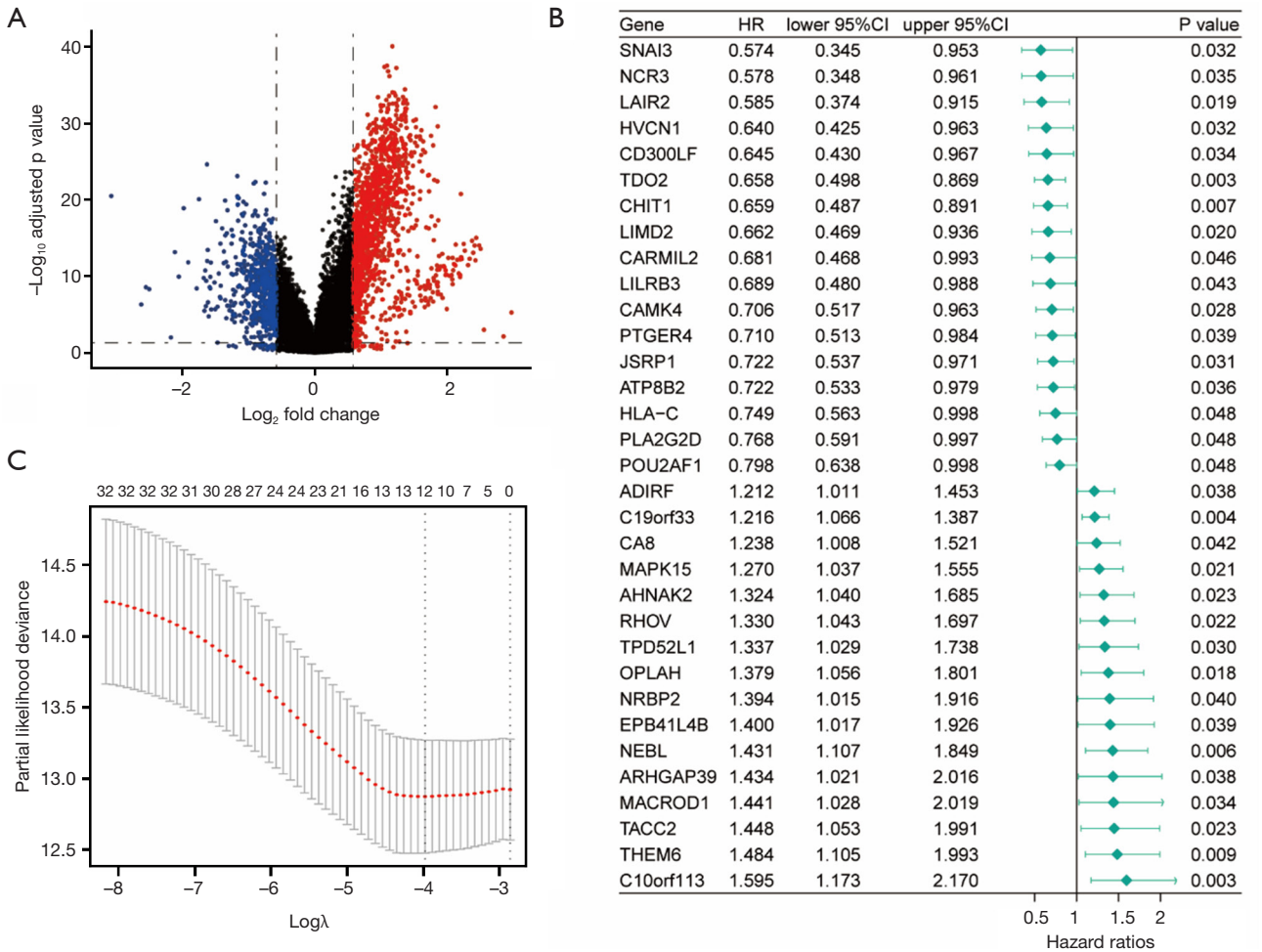

Figure 2 Identification of differentially expressed IRGs and construction of prognostic model. (A) Volcano plot of IRGs in the IM subtype and other subtypes. Through differential expression analysis, downregulated genes are labeled in blue and upregulated genes are labeled in red, respectively. (B) An analysis of univariate regression revealed 33 genes that were linked to prognosis (P<0.05). (C) The LASSO Cox regression model was used to plot partial likelihood deviations against log(λ). HR, hazard ratio; CI, confidence interval; IRGs, immune-related genes; IM, immunomodulatory; LASSO, least absolute shrinkage and selection operator.

solely utilizing pathologic T stage for prognosis prediction, the anticipated AUC values for the 1-, 3-, and 5-year operating curves in the training and validation sets were 0.50, 0.55, and 0.54 and 0.78, 0.74, and 0.68, respectively (Figure S1A,S1B). Using only the pathologic N stage as a predictor of prognosis, the predicted AUC values for the 1-, 3-, and 5-year operating curves in the training and validation sets were 0.74, 0.74, and 0.70 and 0.82, 0.77, and 0.74, respectively (Figure S1C,S1D). Moreover, when we integrated the risk score with pathologic T and N stage to forecast prognosis, the projected AUC values for the 1-, 3-, and 5-year operating curves in the training and validation sets were 0.78, 0.83, and 0.75 and 0.91, 0.85, and 0.81, respectively (*Figure 4B*). The calibration graph additionally demonstrated that the forecast likelihood of the nomogram aligned with the real probability of RFS at 1, 3, and 5 years (*Figure 4C*), demonstrating the model's prediction ability with satisfactory discrimination and accuracy.

Molecular features of the high- and low-risk groups

Prognostic genes were identified by conducting differential expression analysis between the high-risk and low-risk groups. A total of 885 distinct genes with differential expression (P<0.05, |log FC| >0.58) between the high-risk and low-risk groups were identified. The results of the

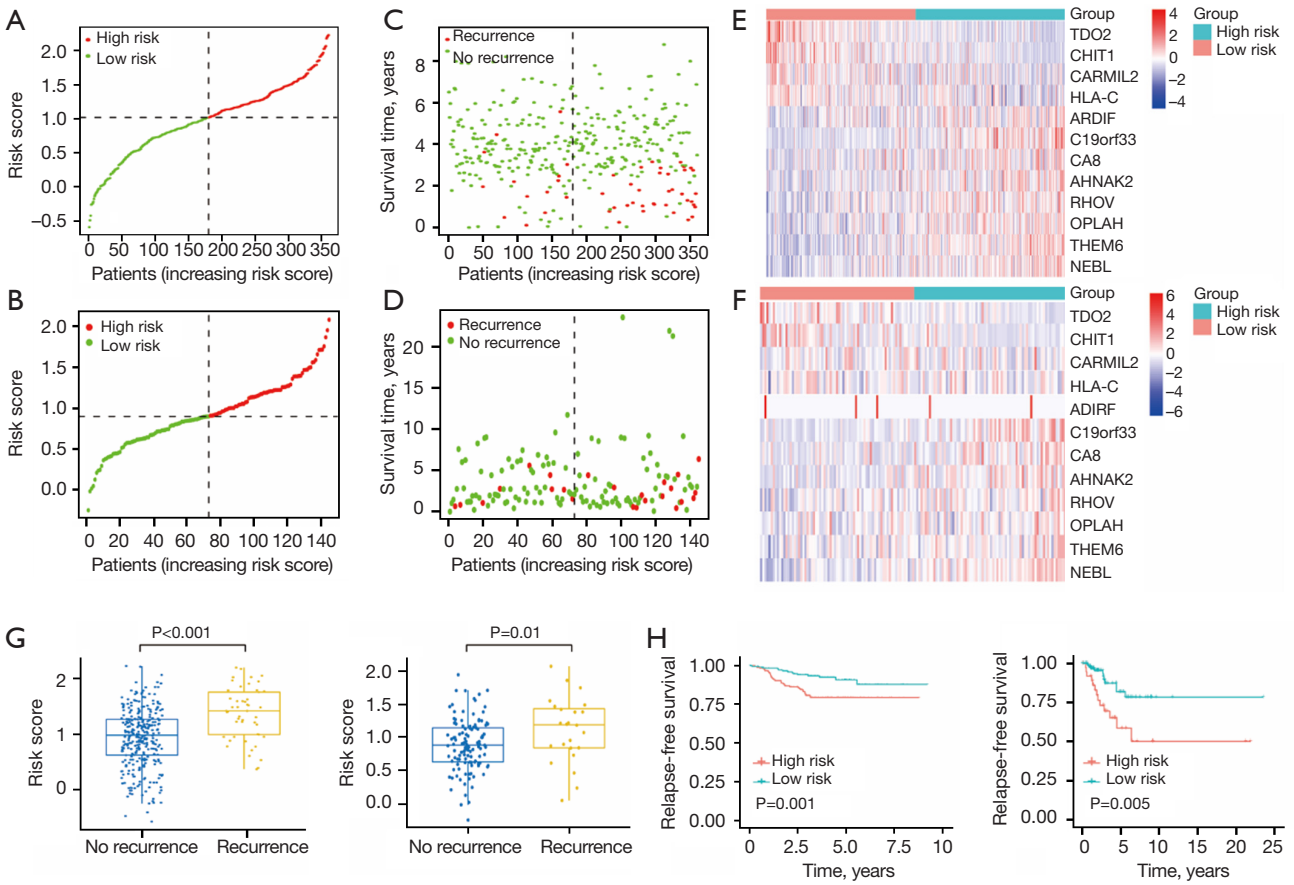

Figure 3 Validation of prognostic risk scoring model. (A) An illustration of the distribution of risk scores in the FUSCC TNBC cohort is shown below. The color progression from green to red indicates the progression from low- to high-risk scores. (B) TCGA TNBC cohort risk score distribution. Low risk is indicated by the color green, while high risk is indicated by the color red. (C) The FUSCC TNBC cohort includes information about the survival status and duration of survival for each patient with TNBC. (D) Survival status and survival time were examined for patients in the TCGA TNBC group. (E) The FUSCC TNBC cohort displays a heatmap illustrating the expression of 12 immune-related genes that are prognostic for TNBC patients. (F) The TCGA TNBC cohort displays a heatmap illustrating the expression of 12 immune-related genes that are prognostic for TNBC patients. (G) Risk score in the no recurrence and recurrence groups in the FUSCC TNBC (left) and TCGA TNBC cohorts (right). Comparison using an unpaired *t*-test. (H) The survival rates of patients with TNBC in the high-risk and low-risk groups were compared in the FUSCC TNBC cohort (on the left) and the TCGA TNBC cohort (on the right). Statistical tests were performed using the log rank method. FUSCC, Fudan University Shanghai Cancer Center; TNBC, triple-negative breast cancer; TCGA, The Cancer Genome Atlas.

enrichment analysis for biological process (BP) indicated that the differentially expressed genes were primarily enriched in the promotion of leukocyte activation and cell activation (*Figure 5A*). The results of the enrichment analysis for cell component (CC) indicated that the immunoglobulin complex and the external side of the plasma membrane were the main areas where differentially expressed genes were enriched (*Figure 5B*). The results of the analysis on molecular functions (MFs) indicated that various genes with differential expression were primarily enriched in antigen binding and binding to immunoglobulin receptors (*Figure 5C*). The KEGG pathway enrichment analysis showed that the genes with differential expression were predominantly enriched in cell adhesion molecules and infection caused by *Staphylococcus aureus* (*Figure 5D*). Next, we conducted additional analysis on the impacts of genetic mutations in both the high-risk and low-risk groups (Figure S2A,S2B). The top 15 genes with the

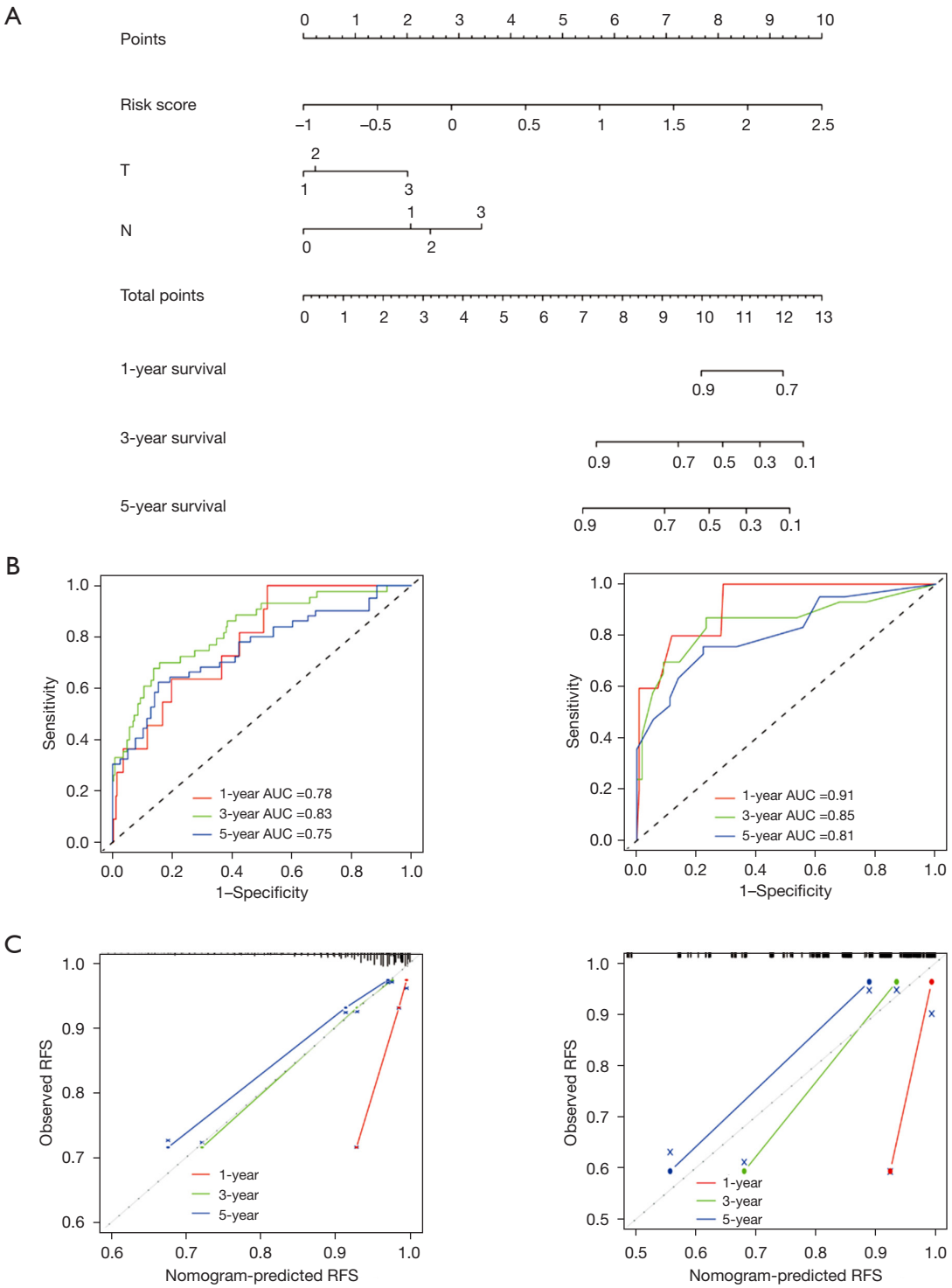

Figure 4 Combination of risk score and clinicpathological features to improve risk stratification and survival prediction. (A) A nomogram that merges a risk score with clinical attributes. (B) The time-ROC curves of the risk score combined with T and N stage in the FUSCC TNBC (left) and TCGA TNBC (right) cohorts. (C) Calibration plots of the risk score combined with clinicopathological features in the FUSCC TNBC (left) and TCGA TNBC (right) cohorts. AUC, area under the curve; RFS, recurrence-free survival; ROC, receiver operator characteristic; FUSCC, Fudan University Shanghai Cancer Center, TNBC, triple-negative breast cancer; TCGA, The Cancer Genome Atlas; T, tumor; N, lymph node.

highest mutation frequencies were identified. In the low-risk group, the *TP53*, *PIK3CA*, *TTN*, *KMT2C*, and *ABCA13* genes exhibited the most frequent mutations. In the high-risk group, the *TP53*, *TTN*, *PIK3CA*, *MUC16*, and *OBSCN* genes exhibited the most mutations.

Differences between high-risk and low-risk groups in terms of immunity

Our calculation of immune infiltration percentages based on the LM22 signature matrix was performed using CIBERSORT, and the integration of CIBERSORT and differential expression profiling revealed an abundance of immune-activated cells and immunostimulators within the low-risk group (*Figure 5E* and Figure S3A) (21,23). Meanwhile, we found that the low-risk group had a significant increase in the expression of immunoinhibitors, which further supports the use of immune checkpoint blockade as a therapeutic strategy (Figure S3B) (23).

To examine the association between IRGs and the effectiveness of immunotherapy, a total of 29 patients who received neoadjuvant immunotherapy in conjunction with chemotherapy were included in the study. The findings indicated that *TDO2* and *HLA-C* exhibited reduced expression in non-pCR individuals (n=10). Conversely, *OPLAH* was overexpressed in non-pCR patients (*Figure 6*). The utilization of these genes is anticipated for the prediction of the clinical effectiveness of TNBC immunotherapy.

Single-cell RNA-seq analysis of 12 genes of the signature

Using the tSNE technique and Single R annotation, we categorized TNBC tumor cells and microenvironmental cells from five patients in the GEO (GSE148673) repository. Our analysis revealed eight distinct cell clusters comprising malignant cells, B cells, T cells, macrophages, monocytes, fibroblasts, endothelial cells, and tissue stem cells (*Figure 7A*). The expression of the 12 genes in the signature revealed that *HLA-C*, *ADIRF*, *C19orf33*, *CA8*, *AHNAK2*, *RHOV*, *OPLAH*, *THEM6*, and *NEBL* were frequently expressed in tumor cells, as depicted in *Figure 7B-7M*. However, *TDO2*, *CHIT1*, and *CARMIL2* had higher expression in tumor stem cells, macrophages and T cells, respectively. In addition, consistent with previous studies (24,25), we observed that *HLA-C* was expressed at a high level in all other immune cells. In addition, the Dim plot illustrates the relative expression of the 12 genes in the signatures (*Figure 7N*).

Discussion

In our prior investigation, we categorized TNBCs into four transcriptome-derived subcategories: (I) luminal androgen receptor (LAR), (II) IM, (III) immune-suppressed basal-like, and (IV) mesenchymal-like. Among each subtype, we discovered potential therapeutic targets or biomarkers (16). For this research, we incorporated 360 individuals with TNBC from the FUSCC TNBC group and discovered 2008 different expression genes (DEGs) between IM and the remaining subtypes, which were selected for subsequent investigation. Potential prognostic factors were identified through regression analysis, revealing 12 immune-related DEGs (*TDO2*, *CHIT1*, *CARMIL2*, *HLA-C*, *ADIRF*, *C19orf33*, *CA8*, *AHNAK2*, *RHOV*, *OPLAH*, *THEM6*, and *NEBL*). A risk score model was constructed using these genetic factors, enabling accurate prediction of RFS in patients with TNBC. Furthermore, the validation of the model was conducted using a dataset acquired from the TCGA TNBC cohort, suggesting its potential broad applicability for patients with TNBC.

According to our discovery, the risk-scoring model consisting of 12 genes has the potential to be used as a prognostic predictor for TNBC. Notably, *TDO2*, *CHIT1*, *CARMIL2*, and *HLA-C* were identified as protective factors that contribute to a favorable prognosis. *ADIRF*, *C19orf33*, *CA8*, *AHNAK2*, *RHOV*, *OPLAH*, *THEM6* and *NEBL* were risk factors unfavorable to prognosis. *TDO2* participates in the metabolism of tryptophan (26), catalyzing the production of kynurenine, which undermines the immune surveillance of the host and facilitates the progression of cancer (27). *CHIT1*, also known as chitotriosidase, is a member of the GH18 glycosyl hydrolase family 18 in humans (28,29). A prior investigation indicated that *CHIT1* levels are increased in individuals diagnosed with primary breast cancer (30). Invadopodia formation necessitates the presence of *CARMIL2*, a regulator of capping protein and linker of myosin 1 (31). Impaired T-cell activation has been reported as a characteristic of *CARMIL2* deficiency (32). The *HLA-C* gene is part of the major histocompatibility complex and has become a prominent target of biomedical research due to its involvement in a number of diseases, such as cancer and autoimmune disorders (33-36). Studies have demonstrated variations in *C10orf116* among various pathological grades of ovarian carcinoma and nonmuscle-invasive bladder cancer (37-39). *C10orf116* deficiency in

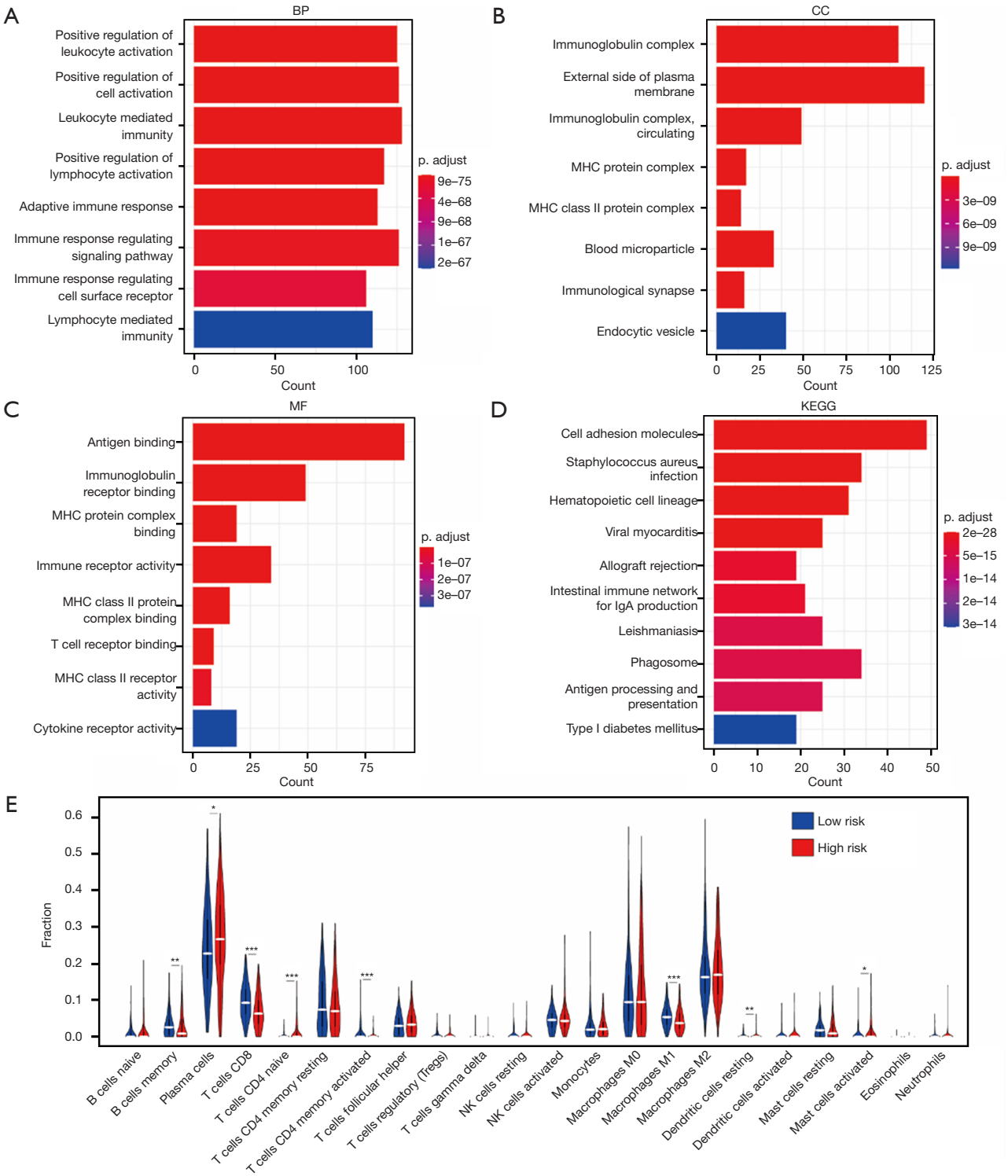

Figure 5 Molecular features of the high- and low-risk groups. (A-D) Enrichment analysis for differentially expressed genes in the high- and low-risk groups was performed using (A-D). BP (A), CC (B), MF (C), and KEGG (D) methods. (E) The proportions of infiltrating immune cells across different risk groups are illustrated by the Violin plot. Comparison using an unpaired *t*-test. Significant results were observed at ***, P<0.001; **, P<0.01, and *, P<0.05, respectively. BP, biological process; CC, cell component; MF, molecular function; KEGG, Kyoto Encyclopedia of Genes and Genomes.

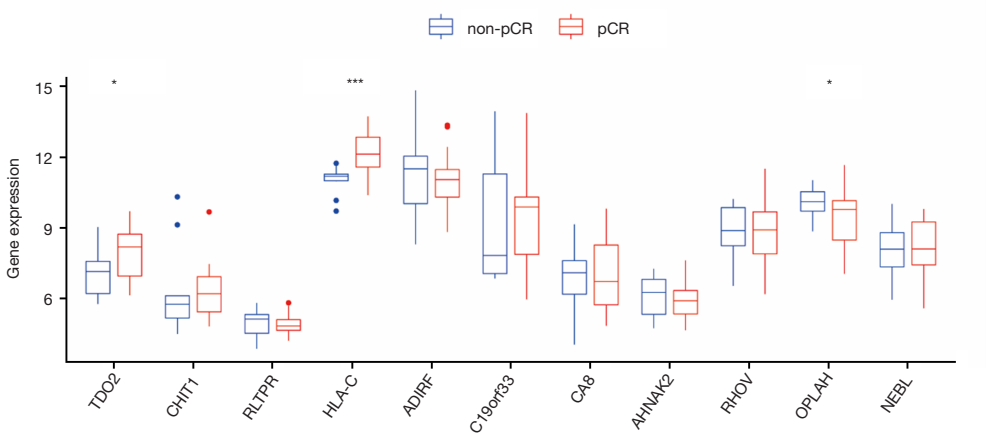

Figure 6 Correlation between IRGs expression and the efficacy of immunotherapy. Comparison using an unpaired *t*-test. Significant results were observed at ***, P<0.001; and *, P<0.05, respectively. pCR, pathologic complete response; IRGs, immune-related genes.

prostate cancer (PCa) is linked to unfavorable disease-free-survival (DFS) outcomes (37). Pancreatic cancer, along with other types of cancer, has been found to exhibit abnormal expression of *C19orf33* in previous research (40). According to reports, the excessive expression of *CA8* has been found to enhance the proliferative and migratory capabilities of renal cell carcinoma (RCC) (41). In thyroid carcinoma tissues, *AHNAK2* was discovered to be increased, and it stimulates the advancement of thyroid carcinoma by activating the NF-κB pathway (42). According to a recent investigation, it was suggested that *RHOV* enhances the growth and spread of lung adenocarcinoma cells via the JNK/c-Jun pathway (43). Earlier research indicated that *OPLAH* functions as a standalone prognostic factor for gastric cancer and squamous cell carcinoma, as evidenced by previous studies (44,45). In a prior investigation, it was discovered that *THEM6*, a member of the thioesterase superfamily, serves as an indicator of resistance to ADT in PCa (46). According to prior research, *NEBL* has been identified as a crucial element in the advancement of ovarian cancer (47). These genes, as indicated by the aforementioned studies, might have an impact on the advancement of TNBC. Furthermore, immune-associated DEGs have the capability to accurately forecast the outcomes of patients with TNBC.

In addition to accurately predicting tumor progression and prognosis, the risk score more effectively distinguishes immune cells infiltrating TNBC from nontumor cells. The low-risk group exhibited notably elevated levels of infiltration by *CD8*$^+$ T cells, *CD4* memory-activated T cells, and M1 macrophages. *CD8*$^+$ T cells play a significant role in the immune response by identifying and acknowledging tumor cells in tumor immunotherapy (48). In the traditional sense, *CD4*$^+$ T cells are regarded as assisting cells that stimulate *CD8*$^+$ T cells (49,50). Upon different stimuli, uncommitted macrophages (M0) transform into proinflammatory macrophages (M1 and M2), and the production of proinflammatory cytokines by M1 macrophages hinders tumor growth (51,52). To some degree, within the low-risk category, there was a notable increase in the expression of substances that boost the immune system and substances that suppress the immune system, suggesting positive immune responses and advantages of immunotherapy.

Nevertheless, our study still has certain limitations. The predictive model still needs additional validation through extensive clinical trials. Furthermore, it is necessary to conduct biological experiments to investigate the underlying mechanisms of immune-related prognostic genes in TNBC.

Conclusions

In summary, a signature consisting of twelve genes was created by utilizing IRGs that exhibited differential expression between the IM subtype and other subtypes. This signature has been shown to be sufficiently accurate to predict prognosis in TNBC patients. In addition, the signature is linked to the expression of immune checkpoints and the infiltration of immune cells, providing a means to identify potential populations that could potentially benefit from immunotherapy.

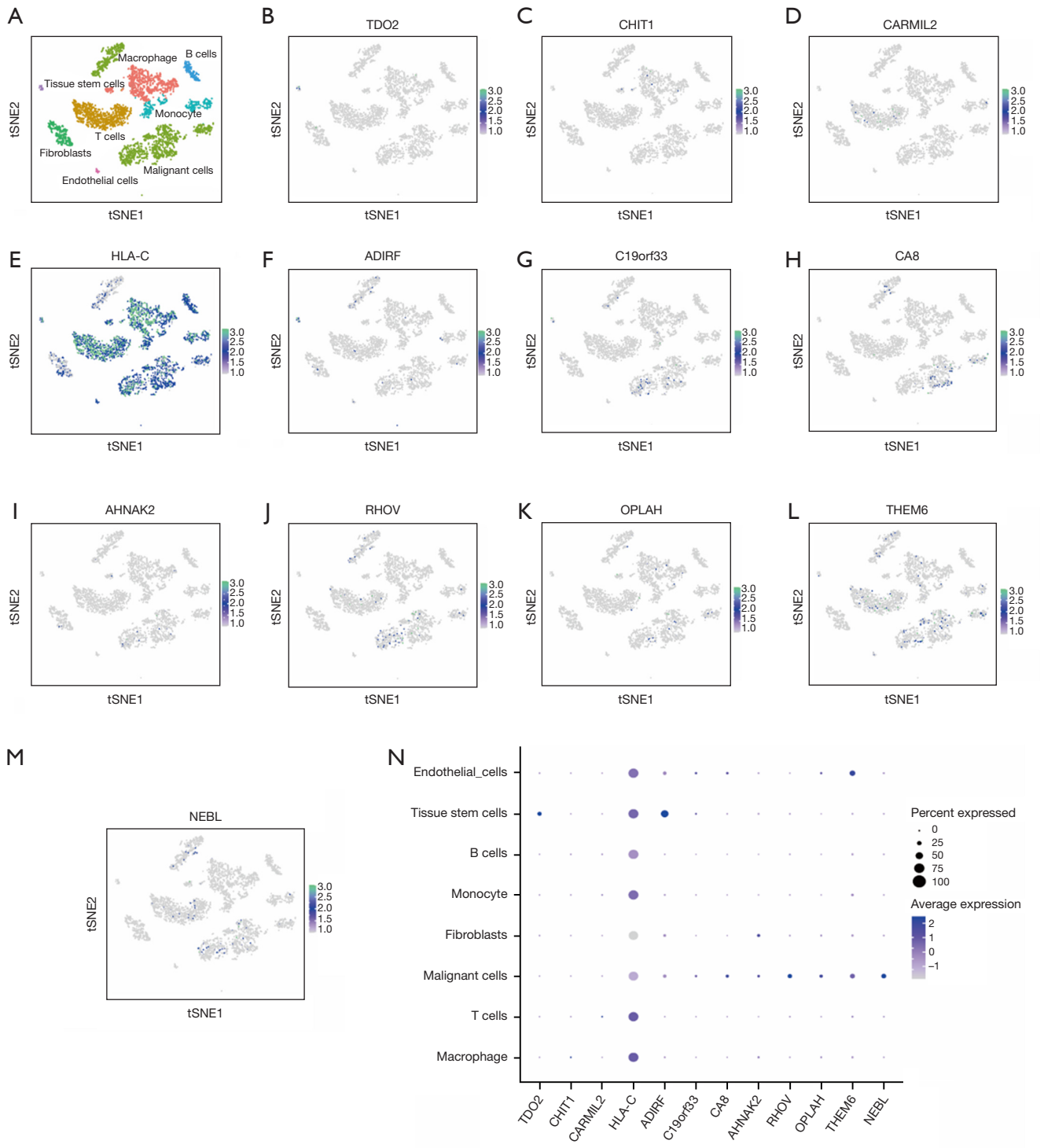

Figure 7 Single-cell RNA-seq analysis of 12 IRGs. (A) Distribution of cell clusters shown by the tSNE method. (B-M) The mRNA expression of (B) *TDO2*, (C) *CHIT1*, (D) *CARMIL2*, (E) *HLA-C*, (F) *ADIRF*, (G) *C19orf33*, (H) *CA8*, (I) *AHNAK2*, (J) *RHOV*, (K) *OPLAH*, (L) *THEM6*, and (M) *NEBL* in different cell clusters. (N) Dim plot of gene distribution. IRGs, immune-related genes; tSNE, t-distributed Stochastic Neighbor Embedding.

Acknowledgments

We are grateful to the AJE platform for checking and modifying the language. We also thank Dr. Yang Ouyang and Xi-Yi Sui for editing the manuscript.
Funding: None.

Footnote

Reporting Checklist: The authors have completed the TRIPOD reporting checklist. Available at https://tcr.amegroups.com/article/view/10.21037/tcr-23-1554/rc

Data Sharing Statement: Available at https://tcr.amegroups.com/article/view/10.21037/tcr-23-1554/dss

Peer Review File: Available at https://tcr.amegroups.com/article/view/10.21037/tcr-23-1554/prf

Conflicts of Interest: Both authors have completed the ICMJE uniform disclosure form (available at https://tcr.amegroups.com/article/view/10.21037/tcr-23-1554/coif). The authors have no conflicts of interest to declare.

Ethical Statement: The authors are accountable for all aspects of the work in ensuring that questions related to the accuracy or integrity of any part of the work are appropriately investigated and resolved. The study was conducted in accordance with the Declaration of Helsinki (as revised in 2013). The study was approved by the independent ethics committee at Fudan University Shanghai Cancer Center Ethical Committee (No. 2019171). Informed consent were obtained.

References

1. Kamangar F, Dores GM, Anderson WF. Patterns of Cancer Incidence, Mortality, and Prevalence Across Five Continents: Defining Priorities to Reduce Cancer Disparities in Different Geographic Regions of the World. J Clin Oncol 2023;41:5209-24.
2. Chong W, Zhang H, Guo Z, et al. Aquaporin 1 promotes sensitivity of anthracycline chemotherapy in breast cancer by inhibiting β-catenin degradation to enhance TopoIIα activity. Cell Death Differ 2021;28:382-400.
3. Grinda T, Antoine A, Jacot W, et al. Evolution of overall survival and receipt of new therapies by subtype among 20 446 metastatic breast cancer patients in the 2008-2017 ESME cohort. ESMO Open 2021;6:100114.
4. Dri A, Arpino G, Bianchini G, et al. Breaking barriers in triple negative breast cancer (TNBC) - Unleashing the power of antibody-drug conjugates (ADCs). Cancer Treat Rev 2024;123:102672.
5. Bianchini G, De Angelis C, Licata L, et al. Treatment landscape of triple-negative breast cancer - expanded options, evolving needs. Nat Rev Clin Oncol 2022;19:91-113.
6. Bauer KR, Brown M, Cress RD, et al. Descriptive analysis of estrogen receptor (ER)-negative, progesterone receptor (PR)-negative, and HER2-negative invasive breast cancer, the so-called triple-negative phenotype: a population-based study from the California cancer Registry. Cancer 2007;109:1721-8.
7. De Laurentiis M, Cianniello D, Caputo R, et al. Treatment of triple negative breast cancer (TNBC): current options and future perspectives. Cancer Treat Rev 2010;36 Suppl 3:S80-6.
8. Rizzo A, Cusmai A, Acquafredda S, et al. Ladiratuzumab vedotin for metastatic triple negative cancer: preliminary results, key challenges, and clinical potential. Expert Opin Investig Drugs 2022;31:495-8.
9. Rizzo A, Ricci AD, Lanotte L, et al. Immune-based combinations for metastatic triple negative breast cancer in clinical trials: current knowledge and therapeutic prospects. Expert Opin Investig Drugs 2022;31:557-65.
10. Santoni M, Rizzo A, Mollica V, et al. The impact of gender on The efficacy of immune checkpoint inhibitors in cancer patients: The MOUSEION-01 study. Crit Rev Oncol Hematol 2022;170:103596.
11. Cortes J, Cescon DW, Rugo HS, et al. Pembrolizumab plus chemotherapy versus placebo plus chemotherapy for previously untreated locally recurrent inoperable or metastatic triple-negative breast cancer (KEYNOTE-355): a randomised, placebo-controlled, double-blind, phase 3 clinical trial. Lancet 2020;396:1817-28.
12. Karn T, Jiang T, Hatzis C, et al. Association Between

Genomic Metrics and Immune Infiltration in Triple-Negative Breast Cancer. JAMA Oncol 2017;3:1707-11.
13. Rizzo A, Ricci AD. Biomarkers for breast cancer immunotherapy: PD-L1, TILs, and beyond. Expert Opin Investig Drugs 2022;31:549-55.
14. Buisseret L, Garaud S, de Wind A, et al. Tumor-infiltrating lymphocyte composition, organization and PD-1/ PD-L1 expression are linked in breast cancer. Oncoimmunology 2016;6:e1257452.
15. Keenan TE, Tolaney SM. Role of Immunotherapy in Triple-Negative Breast Cancer. J Natl Compr Canc Netw 2020;18:479-89.
16. Jiang YZ, Ma D, Suo C, et al. Genomic and Transcriptomic Landscape of Triple-Negative Breast Cancers: Subtypes and Treatment Strategies. Cancer Cell 2019;35:428-440.e5.
17. Harrington D, Parmigiani G. Adaptive Randomization of Neratinib in Early Breast Cancer. N Engl J Med 2016;375:1593-4.
18. Rugo HS, Olopade OI, DeMichele A, et al. Adaptive Randomization of Veliparib-Carboplatin Treatment in Breast Cancer. N Engl J Med 2016;375:23-34.
19. Friedman J, Hastie T, Tibshirani R. Regularization Paths for Generalized Linear Models via Coordinate Descent. J Stat Softw 2010;33:1-22.
20. Kamarudin AN, Cox T, Kolamunnage-Dona R. Time-dependent ROC curve analysis in medical research: current methods and applications. BMC Med Res Methodol 2017;17:53.
21. Newman AM, Liu CL, Green MR, et al. Robust enumeration of cell subsets from tissue expression profiles. Nat Methods 2015;12:453-7.
22. Mayakonda A, Lin DC, Assenov Y, et al. Maftools: efficient and comprehensive analysis of somatic variants in cancer. Genome Res 2018;28:1747-56.
23. Angelova M, Charoentong P, Hackl H, et al. Characterization of the immunophenotypes and antigenomes of colorectal cancers reveals distinct tumor escape mechanisms and novel targets for immunotherapy. Genome Biol 2015;16:64.
24. Anderson SK. Molecular evolution of elements controlling HLA-C expression: Adaptation to a role as a killer-cell immunoglobulin-like receptor ligand regulating natural killer cell function. HLA 2018;92:271-8.
25. Parham P, Moffett A. Variable NK cell receptors and their MHC class I ligands in immunity, reproduction and human evolution. Nat Rev Immunol 2013;13:133-44.
26. Wang R, Yu Z, Chen F, et al. miR-300 regulates the epithelial-mesenchymal transition and invasion of hepatocellular carcinoma by targeting the FAK/ PI3K/AKT signaling pathway. Biomed Pharmacother 2018;103:1632-42.
27. Miyazaki T, Chung S, Sakai H, et al. Stemness and immune evasion conferred by the TDO2-AHR pathway are associated with liver metastasis of colon cancer. Cancer Sci 2022;113:170-81.
28. Sun S, Li J, Wang S, et al. CHIT1-positive microglia drive motor neuron ageing in the primate spinal cord. Nature 2023;624:611-20.
29. Fadel F, Zhao Y, Cachau R, et al. New insights into the enzymatic mechanism of human chitotriosidase (CHIT1) catalytic domain by atomic resolution X-ray diffraction and hybrid QM/MM. Acta Crystallogr D Biol Crystallogr 2015;71:1455-70.
30. Thein MS, Kohli A, Ram R, et al. Chitotriosidase, a marker of innate immunity, is elevated in patients with primary breast cancer. Cancer Biomark 2017;19:383-91.
31. Lanier MH, Kim T, Cooper JA. CARMIL2 is a novel molecular connection between vimentin and actin essential for cell migration and invadopodia formation. Mol Biol Cell 2015;26:4577-88.
32. Shamriz O, Simon AJ, Lev A, et al. Exogenous interleukin-2 can rescue in-vitro T cell activation and proliferation in patients with a novel capping protein regulator and myosin 1 linker 2 mutation. Clin Exp Immunol 2020;200:215-27.
33. Vollmers S, Lobermeyer A, Körner C. The New Kid on the Block: HLA-C, a Key Regulator of Natural Killer Cells in Viral Immunity. Cells 2021;10:3108.
34. Liu B, Shao Y, Fu R. Current research status of HLA in immune-related diseases. Immun Inflamm Dis 2021;9:340-50.
35. Long EO. Tumor cell recognition by natural killer cells. Semin Cancer Biol 2002;12:57-61.
36. Cooley S, Parham P, Miller JS. Strategies to activate NK cells to prevent relapse and induce remission following hematopoietic stem cell transplantation. Blood 2018;131:1053-62.
37. Meng J, Wang LH, Zou CL, et al. C10orf116 Gene Copy Number Loss in Prostate Cancer: Clinicopathological Correlations and Prognostic Significance. Med Sci Monit 2017;23:5176-83.
38. Marín-Aguilera M, Mengual L, Ribal MJ, et al. Utility of urothelial mRNA markers in blood for staging and monitoring bladder cancer. Urology 2012;79:240.e9-15.
39. Skubitz AP, Pambuccian SE, Argenta PA, et al. Differential

gene expression identifies subgroups of ovarian carcinoma. Transl Res 2006;148:223-48.
40. Zhang M, Zhu J, Zhang P, et al. Development and validation of cancer-associated fibroblasts-related gene landscape in prognosis and immune microenvironment of bladder cancer. Front Oncol 2023;13:1174252.
41. Ma HL, Yu SJ, Chen J, et al. CA8 promotes RCC proliferation and migration though its expression level is lower in tumor compared to adjacent normal tissue. Biomed Pharmacother 2020;121:109578.
42. Ye R, Liu D, Guan H, et al. AHNAK2 promotes thyroid carcinoma progression by activating the NF-κB pathway. Life Sci 2021;286:120032.
43. Zhang D, Jiang Q, Ge X, et al. RHOV promotes lung adenocarcinoma cell growth and metastasis through JNK/c-Jun pathway. Int J Biol Sci 2021;17:2622-32.
44. Wen F, Huang J, Lu X, et al. Identification and prognostic value of metabolism-related genes in gastric cancer. Aging (Albany NY) 2020;12:17647-61.
45. Shimizu D, Kanda M, Kishida T, et al. OPLAH Protein Expression Stratifies the Prognosis of Patients With Squamous Cell Carcinoma of the Esophagus. Cancer Genomics Proteomics 2023;20:343-53.
46. Blomme A, Peter C, Mui E, et al. THEM6-mediated reprogramming of lipid metabolism supports treatment resistance in prostate cancer. EMBO Mol Med 2022;14:e14764.
47. Na Z, Fan L, Wang X. Gene Signatures and Prognostic Values of N6-Methyladenosine Related Genes in Ovarian Cancer. Front Genet 2021;12:542457.
48. Kim HJ, Cantor H. CD4 T-cell subsets and tumor immunity: the helpful and the not-so-helpful. Cancer Immunol Res 2014;2:91-8.
49. Bourgeois C, Rocha B, Tanchot C. A role for CD40 expression on CD8+ T cells in the generation of CD8+ T cell memory. Science 2002;297:2060-3.
50. Mackey MF, Barth RJ Jr, Noelle RJ. The role of CD40/CD154 interactions in the priming, differentiation, and effector function of helper and cytotoxic T cells. J Leukoc Biol 1998;63:418-28.
51. Wu Z, Bai Y, Qi Y, et al. HDAC1 disrupts the tricarboxylic acid (TCA) cycle through the deacetylation of Nur77 and promotes inflammation in ischemia-reperfusion mice. Cell Death Discov 2023;9:10.
52. Mills CD. Anatomy of a discovery: m1 and m2 macrophages. Front Immunol 2015;6:212.

Cite this article as: Song XQ, Shao ZM. Identification of immune-related prognostic biomarkers in triple-negative breast cancer. Transl Cancer Res 2024;13(4):1707-1720. doi: 10.21037/tcr-23-1554

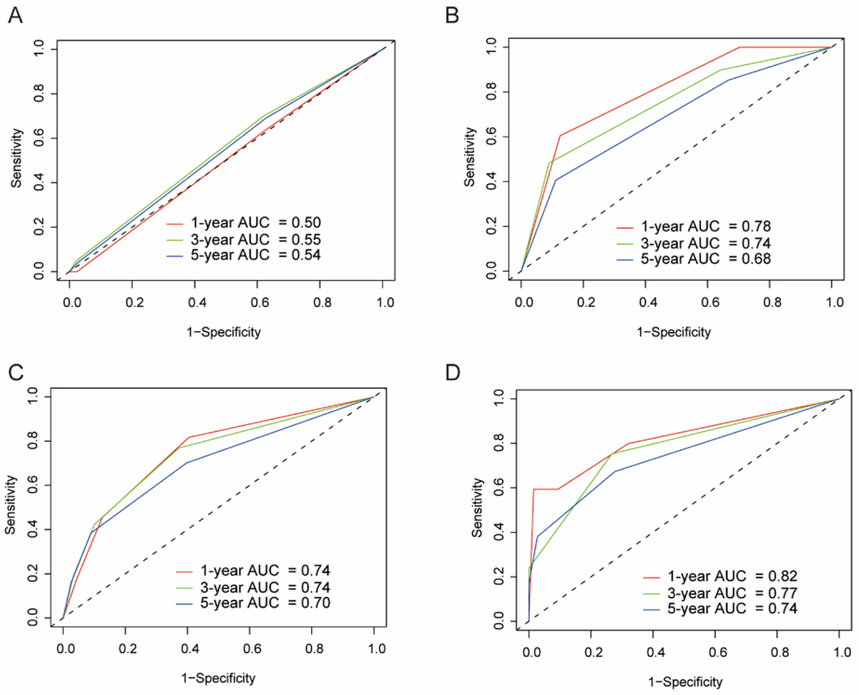

Figure S1 The time-ROC curve for evaluating prognosis. The time-ROC curves of T (A) and N (C) in the FUSCC TNBC cohort. The time-ROC curves of T (B) and N (D) in the TCGA TNBC cohort. ROC, receiver operator characteristic; FUSCC, Fudan University Shanghai Cancer Center, TNBC, Triple-negative breast cancer; TCGA, The Cancer Genome Atlas; T, tumor; N, lymph node.

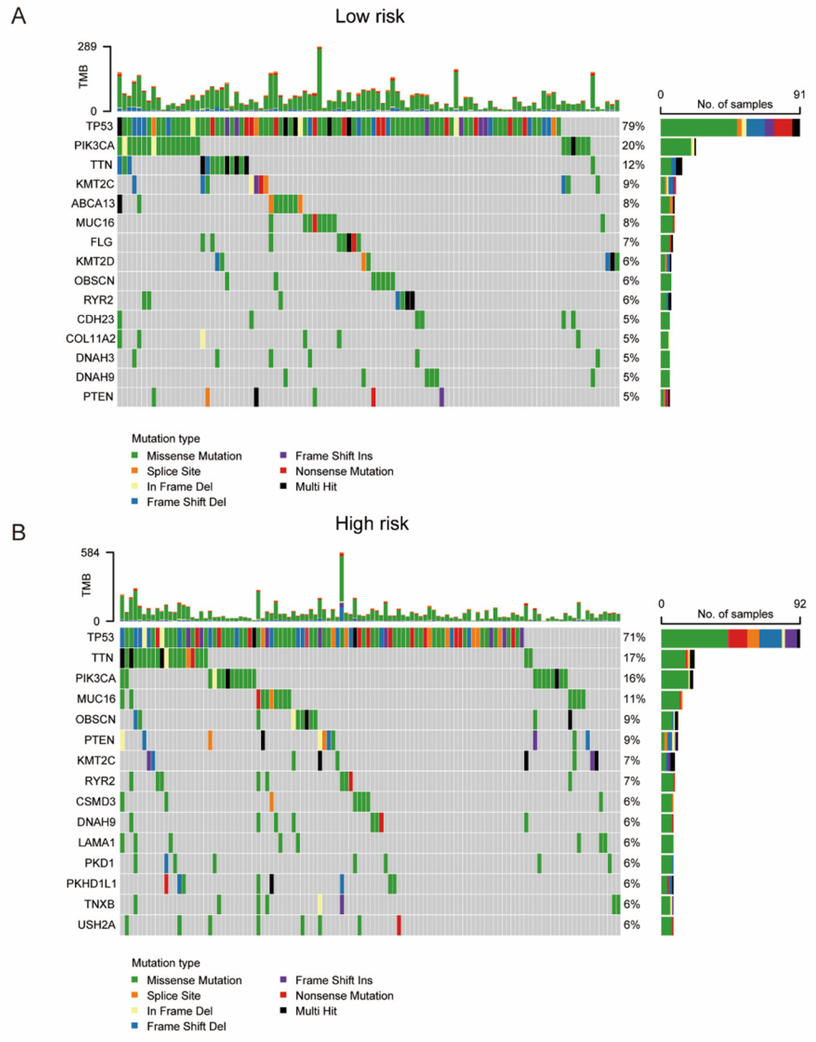

).21037/tcr-23-1554

Figure S2 The landscape of genetic mutations of high- and low-risk groups. (A,B) The waterfall diagram displays the mutation specifics and tumor mutation burden for every sample of TNBC cancer patients in the low-risk (A) and high-risk (B) categories. TNBC, Triple-negative breast cancer.

 https://dx.doi.org/10.21037/tcr-23-1554

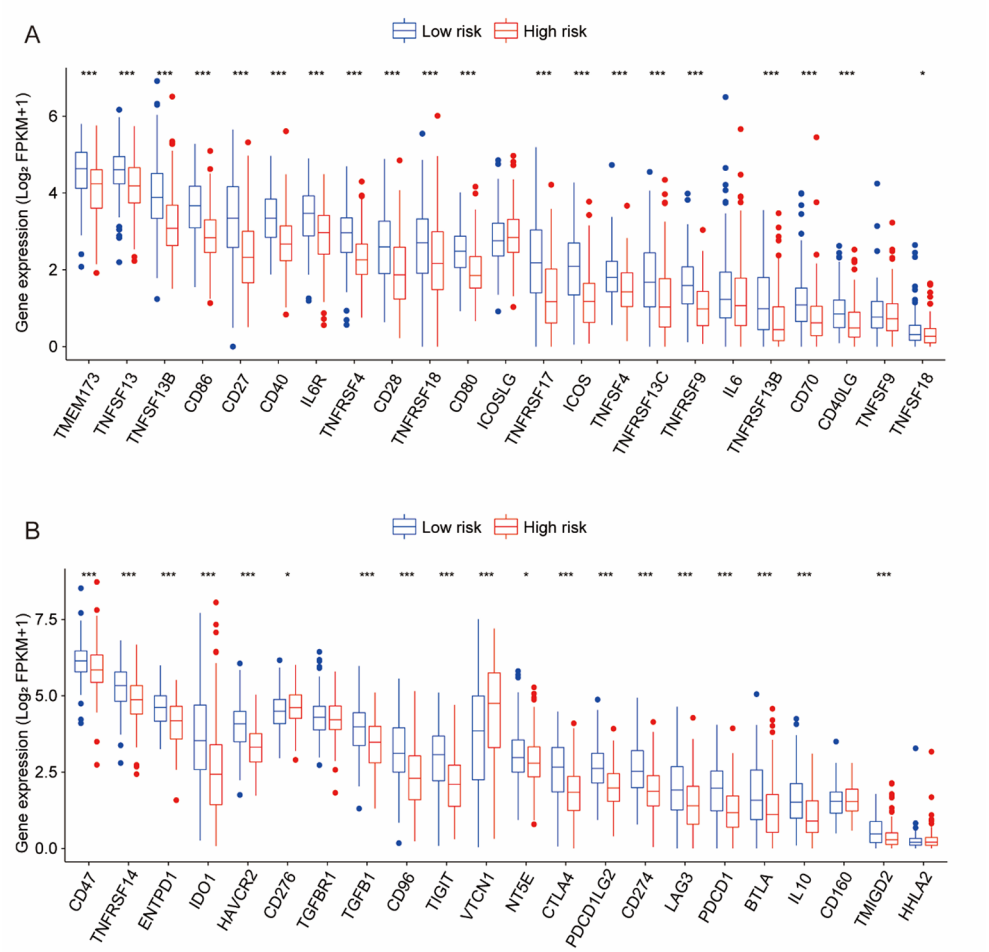

Figure S3 The immune landscape of high- and low-risk groups. (A) The presence of immune-boosting substances in individuals classified as high- and low-risk. (B) The high- and low-risk groups exhibited differential expression of immune checkpoint genes. Comparison using an unpaired *t*-test. Significant results were observed at P<0.001, and P<0.05, denoted as *** and *, respectively.

https://dx.doi.org/10.21037/tcr-23-1554